

University of Nebraska - Lincoln  
**DigitalCommons@University of Nebraska - Lincoln**

---

Robert Powers Publications

Published Research - Department of Chemistry

---

2013

## Multivariate Analysis in Metabolomics

Bradley Worley

*University of Nebraska-Lincoln*, [bradley.worley@huskers.unl.edu](mailto:bradley.worley@huskers.unl.edu)

Robert Powers

*University of Nebraska-Lincoln*, [rpowers3@unl.edu](mailto:rpowers3@unl.edu)

Follow this and additional works at: <http://digitalcommons.unl.edu/chemistrypowers>

---

Worley, Bradley and Powers, Robert, "Multivariate Analysis in Metabolomics" (2013). *Robert Powers Publications*. 35.  
<http://digitalcommons.unl.edu/chemistrypowers/35>

This Article is brought to you for free and open access by the Published Research - Department of Chemistry at DigitalCommons@University of Nebraska - Lincoln. It has been accepted for inclusion in Robert Powers Publications by an authorized administrator of DigitalCommons@University of Nebraska - Lincoln.



Published in final edited form as:

*Curr Metabolomics*. 2013 ; 1(1): 92–107. doi:10.2174/2213235X11301010092.

© 2013 Bentham Science Publishers. Used by permission.

## Multivariate Analysis in Metabolomics

**Bradley Worley and Robert Powers\***

Department of Chemistry, University of Nebraska-Lincoln, Lincoln, NE 68588-0304

### Abstract

Metabolomics aims to provide a global snapshot of all small-molecule metabolites in cells and biological fluids, free of observational biases inherent to more focused studies of metabolism. However, the staggeringly high information content of such global analyses introduces a challenge of its own; efficiently forming biologically relevant conclusions from any given metabolomics dataset indeed requires specialized forms of data analysis. One approach to finding meaning in metabolomics datasets involves multivariate analysis (MVA) methods such as principal component analysis (PCA) and partial least squares projection to latent structures (PLS), where spectral features contributing most to variation or separation are identified for further analysis. However, as with any mathematical treatment, these methods are not a panacea; this review discusses the use of multivariate analysis for metabolomics, as well as common pitfalls and misconceptions.

### Keywords

Multivariate analysis; PCA; PLS-DA; OPLS-DA; metabolomics; metabonomics

### Introduction

Metabolomics is defined [1] as “the quantitative measurement of the multiparametric metabolic response of living systems to pathophysiological stimuli or genetic modification.” Such a definition implies that metabolomic studies offer the finest-grained detail available in the nascent field of systems biology: a molecular-level convolution of all upstream genomic, transcriptomic and proteomic responses of an organism to a given stimulus or change [2-4]. Metabolites are the end product of all cellular processes, and are a direct outcome of enzymatic and protein activity. Thus, metabolites are more proximal to a phenotype or disease than either genetic or proteomic information [5, 6]. This occurs because a simple change in the expression level of a gene or protein does not necessarily correlate directly with a variation in the activity level of a protein, but an alteration in a metabolite only occurs through such a change [7]. Consequently, metabolomics has been used to identify disease biomarkers [8, 9], to aid in the drug discovery process [10, 11], and to study plants [12], bacteria [13, 14], nutrition [15], and the environment [16], among numerous other applications [17].

\*To whom correspondence should be addressed: Robert Powers, University of Nebraska-Lincoln, Department of Chemistry, 722 Hamilton Hall, Lincoln, NE 68588-0304, rpowers3@unl.edu, Phone: (402) 472-3039, Fax: (402) 472-9402.

However, metabolomics experiments are plagued with difficulty. The number of small-molecule metabolites in a biofluid, cell lysate, tissues or organ differs wildly depending on the organism studied, ranging from several hundred to hundreds of thousands [18]. Metabolomics is also a relatively new discipline and as a result a complete catalog of the human metabolome and the metabolomes of other organisms is not available [19]. Therefore, it is common to encounter unknown metabolites, a complication in the analysis and interpretation of metabolic changes. Similarly, the lack of reference NMR or MS spectra for all known metabolites makes proper identification of metabolites challenging [20-22]. Further, the exhibited diversity of chemical and physical properties of compounds within the metabolome makes true metabolomics (simultaneous quantification of all metabolites) unattainable with current instrumental capabilities [1, 18, 23]. As an illustration, the limited molecular-weight distribution of the metabolome prohibits a comprehensive and detailed analysis by mass spectroscopy and generally requires the additional use of chromatography [2, 24].

The analysis of metabolomic data is further complicated by the inherent variability in each sample. Every single cell, tissue, organ or organism is fundamentally unique [25], despite any defining feature they share in common, such as being the same species, infected with the same disease or receiving the same drug treatment. As such, the overall goal of metabolomics is to identify the few chemical features against a large and complex background of metabolites that uniquely define the system [20, 26]. These few chemical features or metabolites should be directly related to the defining characteristic of the system. But, unfortunately, all biological systems are easily perturbed by any number of experimental or environmental factors, such as age, diet, growth phase, media, nutrients, pH, sex, and temperature [27, 28]. Similarly, cell lysis, enzyme quenching and metabolome extraction techniques, and the storage of the metabolomics samples can also induce undesirable variations. There are also unavoidable fluctuations in spectral data, such as changes in peak position or peak width that are caused by instrument instability and variability in sample conditions. As a result, the analysis of metabolomic data requires a robust methodology to expose underlying trends in these highly complex and variable data sets.

One class of methods, appropriately termed “metabolic fingerprinting,” aims to retain much of the promised unbiased, global nature of the metabolomics experiment by differentially analyzing spectral information acquired from normal and perturbed systems [29]. Again, a perturbed system may result from a disease state, a drug treatment, the presence of a pest or parasite, an environmental stimulus (pH, temperature, toxin, or nutrient change), a temporal, spatial, or species difference. Metabolic fingerprinting is also amenable to high throughput data collection and analysis, since global metabolite profiling can be accomplished with minimal samples and rapid spectral acquisitions [30]. The goal of metabolic fingerprinting experiments is to determine the relative differences between the metabolomes of two or more systems to infer a biological relationship. Thus, a hallmark of metabolic fingerprinting is the use of multivariate analysis methods to identify those biologically relevant spectral features for further targeted analyses [1, 23, 31], with two of the most popular methods being principal component analysis (PCA) [32, 33] and partial least squares projection to latent structures (PLS) [34, 35]. In essence, PCA and PLS aim to differentiate between

classes in highly complex data sets, despite within class variability. These multivariate analysis methods will be briefly described, along with a discussion of their application to metabolomics, with an emphasis on common errors and misconceptions.

### Metabolomics datasets

The choice of analytical method used for metabolic fingerprinting experiments is limited primarily by its ability to reveal metabolic differences due to system perturbations. Other desirable features include minimal sample preparations or requirements, and the ability to analyze the samples in a high-throughput manner. High-resolution  $^1\text{H}$  NMR spectroscopy is especially suited for probing biofluids, cell lysates and tissues with almost no sample treatment and without bias [36, 37]. Mass spectrometry is similarly employed for metabolic fingerprinting and is typically favored for its sensitivity in more global metabolic profiling applications, but generally requires upstream chromatographic separations due to the limited molecular-weight diversity of metabolites [37-39]. Raman and Fourier-transform infrared (FT-IR) spectroscopies have also been successfully utilized [31, 40] for metabolomic studies, and capillary electrophoresis has recently been shown to provide useful data [41, 42] in fingerprinting experiments.

The remarkable diversity of instrumental approaches used in metabolic fingerprinting experiments is traceable in large part to the flexibility of the multivariate analysis techniques used to analyze the collected data. A data matrix  $\mathbf{X}$ , containing  $N$  observation row vectors of  $K$  variables each, is almost universally common [34, 43, 44], and very few mathematical constraints are placed on the values it holds. Correspondingly, NMR, MS, FT-IR, or any other source of spectral data can be used as input into the data matrix  $\mathbf{X}$ . However, as discussed below, preprocessing of the data matrix is essential to yield interpretable results. This data matrix  $\mathbf{X}$  can be immediately decomposed using unsupervised dimensionality reduction methods, such as PCA, or it can be paired with a matrix  $\mathbf{Y}$  of  $N$  corresponding  $M$ -dimensional outputs for use in supervised dimensionality reduction, in the case of PLS regression (PLSR) and its descendants. An output may range from a simple class membership designation [35] to a range of observables [45], such as patient histories (age, sex, weight, etc.). While the same mathematical flexibility also applies to outputs, metabolic fingerprinting data typically stores binary (or  $n$ -ary) class membership information in  $\mathbf{Y}$ , in which case the applicable supervised methods are forms of discriminant analysis (PLS-DA, OPLS-DA). A graphical representation of the data ( $\mathbf{X}$ ) and response ( $\mathbf{Y}$ ) matrices, along with their PCA/PLS decomposition, is shown in Figure 1.

Simply, the primary goal of PCA and PLS is to identify class differences from a multivariate dataset. A class can refer to any biologically relevant classification, such as humans treated with a specific diet or drug; or cells exposed to particular environmental stress (temperature, pH, osmolality, etc.), or different genetic modification to an organism. An NMR, MS, or FT-IR spectrum of a biofluid or metabolome extract is an observation: a vector of  $K$  variables, where each spectrum represents an individual cell culture, tumor or organism. The entire collection of  $N$  observations forms the data matrix  $\mathbf{X}$ . PCA and PLS then identify a combination of the  $K$  variables or spectral features that defines the class separation.

A key characteristic of metabolic fingerprinting datasets is an excess of observed variables ( $K$ ) in comparison to the number of observations ( $N$ ), belonging to the so-called 'large  $K$ , small  $N$ ' class of problems in statistics [46]. This feature makes traditional linear regression methods infeasible, as  $\mathbf{X}$  is no longer invertible (i.e. it is singular) and no unique least-squares solution exists. Consequently, analysis of metabolomics data requires the use of multivariate analysis methods capable of dealing with significant amounts of collinearity in  $\mathbf{X}$ , of which PCA and PLS are prime examples.

### Linear transformations

The ultimate goal of the multivariate dimensionality reduction algorithms discussed herein is to find a  $K$ -by- $P$  matrix  $\mathbf{A}$  that optimally transforms the data matrix  $\mathbf{X}$  into a new matrix of  $P$ -dimensional scores given by  $\mathbf{T}$ :

$$\mathbf{T} = \mathbf{X}\mathbf{A} \quad [1]$$

Thus, each row of  $\mathbf{T}$  is a transformation of the corresponding row of  $\mathbf{X}$ . Alternately, expressing the  $i$ -th row of  $\mathbf{X}$  as a column vector  $\mathbf{x}_i$  and the corresponding row of  $\mathbf{T}$  as a column vector  $\mathbf{t}_i$  shows that the so-called 'weights' matrix  $\mathbf{A}^T$  defines a linear transformation from the input data space occupied by  $\mathbf{X}$  to the output space of  $\mathbf{T}$ , termed the 'scores' space:

$$\mathbf{t}_i = \mathbf{A}^T \mathbf{x}_i \quad [2]$$

In the case where  $P$  is less than  $K$ , the dimensionality of the scores space will be less than that of the input data space and the above transformation has achieved dimensionality reduction. This is a key characteristic of multivariate analysis in metabolic fingerprinting. Finally, the optimal transformation by matrix  $\mathbf{A}$  depends on the chosen algorithm, such as PCA, PLS, or OPLS.

### Principal Component Analysis

Principal component analysis (PCA) is arguably the most widely used multivariate analysis method for metabolic fingerprinting and, in fact, chemometrics in general. The objective of PCA is to arrive at a linear transformation that preserves as much of the variance in the original data as possible in the lower dimensionality output data [44]. It can be shown [44] that the transformation  $\mathbf{A}$  that achieves this objective is a matrix whose columns are the first  $P$  eigenvectors of the non-singular portion of the sample covariance matrix  $\mathbf{S}$ :

$$\mathbf{S} = \frac{1}{N-1} \mathbf{X}^T \mathbf{H} \mathbf{X} = \mathbf{Q} \mathbf{\Lambda} \mathbf{Q}^{-1} \quad [3]$$

Here,  $\mathbf{H}$  is the  $N$ -by- $N$  centering matrix used to center each variable about its sample mean. The second equality above describes the form of the eigendecomposition of  $\mathbf{S}$ , where  $\mathbf{Q}$  is the matrix of eigenvectors of  $\mathbf{S}$  and  $\mathbf{\Lambda}$  is a diagonal matrix of the corresponding eigenvalues. When  $\mathbf{X}$  is left unscaled, the eigenvalues in  $\mathbf{\Lambda}$  equal the variances of the newly transformed

data in  $\mathbf{T}$ , providing a means to calculate the ratio of variance preserved during the transformation relative to the original variance:

$$R_i^2 = \frac{\Lambda_{ii}}{\sum_{j=1}^N S_{jj}} \quad [4]$$

Where  $R_i^2$  is the amount of variance in  $\mathbf{X}$  preserved in the  $i$ -th principal component. Given the fact that  $\Lambda_{ii}$  decreases monotonically with  $i$ , it can be seen that each principal component preserves progressively less variance of the original data.

### Partial Least Squares

While the unsupervised nature of the PCA algorithm provides a means to achieve unbiased dimensionality reduction, its application only reveals group structure when within-group variation is sufficiently less than between-group variation. Therefore, supervised forms of discriminant analysis such as Partial Least Squares (PLS-DA; alternatively Partial Least Squares Projections to Latent Structures [35]) that rely on the class membership of each observation are also commonly applied in metabolic fingerprinting experiments [35, 47]. When class memberships are coded in matrix form into  $\mathbf{Y}$  [47] and the PLS components are constrained to be orthogonal, the dimensionality-reducing transformation  $\mathbf{A}$  is a matrix whose columns are the first  $P$  eigenvectors of a matrix formed by the covariances between  $\mathbf{X}$  and  $\mathbf{Y}$ :

$$\mathbf{S} = \mathbf{S}_{xy} \mathbf{S}_{yx} = \frac{1}{(n-1)^2} \mathbf{X}^T \mathbf{H} \mathbf{Y} \mathbf{Y}^T \mathbf{H} \mathbf{X} \quad [5]$$

Where  $\mathbf{H}$  is again the centering matrix and the eigendecomposition takes an identical form to that shown for PCA. Thus, the new 'latent variables' formed by this transformation are linear combinations of original variables that preserve as much covariance between  $\mathbf{X}$  and  $\mathbf{Y}$  as possible in the first transformed dimensions; simply put, the low-dimensional scores space is formed predominately by the predictive components of  $\mathbf{X}$ . This casting of PLS-DA as an eigendecomposition problem [48] is of course, complementary to the usual description of the algorithm as an iterative regression problem that more closely resembles the roots of PLS regression [34, 35]. However, it provides a means to contrast the results of PLS-DA with those of PCA. In fact, placing every observation into its own class, effectively setting  $\mathbf{Y}$  to the identity, yields an identical eigenvector problem to that of PCA.

It is far more common, however, to find descriptions of PLS-DA that do not impose orthogonality of the PLS components; these methods require instead that the  $\mathbf{X}$  scores be uncorrelated, closer to traditional PLS regression [35]. The popular form of PLS-DA under this condition is then:

$$\mathbf{X} = \widehat{\mathbf{X}} + \mathbf{E} = \mathbf{T} \mathbf{P}^T + \mathbf{E} \quad [6]$$

$$Y = \widehat{Y} + G = UC^T + G \quad [7]$$

Where  $T$  and  $P$  are the scores and loadings for  $X$ ,  $U$  and  $C$  are the scores and loadings for  $Y$ , and  $E$  and  $G$  are the residual errors of  $X$  and  $Y$  that are left unaccounted for in the model. Decomposition is performed such that  $T$  and  $U$  share maximum covariance, in effect allowing  $T$  to serve as an estimator of  $U$ . These equations emphasize the fact that PLS finds a small set of scores and loadings – the latent structures – which most effectively summarize  $X$  and  $Y$  as well as describe their correlation. Until recently, this traditional PLS regression method was referred to as Partial Least Squares due to its use of Non-linear Iterative Partial Least Squares (NIPALS) for estimating model parameters. With the introduction of PLS to chemometrics, an alternative meaning of ‘Projection to Latent Structures’ has also been used for the methods of Partial Least Squares regression [35].

### Orthogonal Projection to Latent Structures

The utilization of class memberships in PLS-DA allows the algorithm to better expose separations between classes in scores space. However, variation not directly correlated with  $Y$  is still present in the scores. This complicates interpretation of PLS-DA scores and loadings plots, especially as the number of classes increases [43]. Orthogonal Projections to Latent Structures (OPLS) addresses this interpretability problem by incorporating an Orthogonal Signal Correction (OSC) filter [49-51] into a PLS model, effectively separating  $Y$ -predictive variation from  $Y$ -uncorrelated variation in  $X$ :

$$X = \widehat{X} + \widehat{X}_o + E = TP^T + T_oP_o^T + E \quad [8]$$

Where  $T_o$  and  $P_o$  are the scores and loadings, respectively, for the  $Y$ -uncorrelated variation identified by the OSC filter. The predictive OPLS-DA scores and loadings used to estimate  $Y$  are then composed of variation directly correlated with  $Y$  and free of interfering structured variation, yielding enhanced interpretability when compared with PLS-DA [43, 52]. Finally, it is important to note that OPLS-DA provides no predictive advantage over PLS-DA [53]; in fact, when no  $Y$ -uncorrelated variation exists in  $X$ , OPLS-DA will yield an identical model to PLS-DA.

### Method Selection

In designing experiments for metabolic fingerprinting studies, the choice of multivariate analysis method must be driven by the data and the experimental goals. For exploratory studies where metabolomic differences between experimental groups may be unknown or unpredictable, initial application of PCA provides an informative first look at the dataset structure and relationships between groups. Even when dataset structure may be predictable, initial use of unbiased methods like PCA provide further confirmation prior to analysis by supervised methods. Ideally, the results of PCA analyses would be used to formulate an initial biological conclusion, which PLS or OPLS can then verify and test in more detail. The principal reason for this is due to the fact that separation is only observed between groups in PCA scores when within-group variation is significantly less than between-group



variation in the data, while separation in PLS scores may simply be fortuitous. Therefore, PLS classification guided by well-separated PCA scores has a greater likelihood of producing biologically relevant results.

## Data Preprocessing

Pre-treatment of raw spectral data is critical for generating reliable, interpretable models using multivariate analysis techniques. A summarization of the procedures involved for preprocessing of metabolic fingerprinting datasets has been well described, and efforts have been made to standardize the processes [54, 55]. Nevertheless, depending on the instrumental technique, the experimenter must adopt certain procedures to obtain an optimal model.

## Binning and alignment

As  $^1\text{H}$  NMR chemical shifts vary at times with a strong dependence on temperature, pH, ionic strength, and other factors that influence their electronic environment, metabolic fingerprinting datasets acquired from NMR spectrometers suffer from imprecisions in chemical shifts, and thus in the  $X$  variables. Therefore, models generated using PCA or PLS-DA on full-resolution  $^1\text{H}$  NMR spectra may fail to identify separations between classes, and their loadings can be difficult to interpret due to the over-abundance of variables. These complications from chemical shift variations may be mitigated by uniformly dividing each spectrum into 'bins' having typical spectral widths of 0.04 ppm and integrating signal intensities within each bin to produce a smaller set of variables. A representative example of a binned  $^1\text{H}$  NMR spectrum is given in Figure 2, showing the appreciable loss of resolution typically incurred.

The binning procedure not only masks subtle chemical shift differences and filters noise in spectra, but it also hides potentially significant changes of low-intensity peaks nearby strong signals. Unfortunately, uniform binning incurs the risk of splitting peaks or spectral features between bins, recreating the imprecision in the  $X$  variables that the preprocessing set out to correct. "Intelligent" or "adaptive" binning endeavors to evade this problem by using variable bin sizes that avoid dividing peaks between multiple bins [56-59]. A recent kernel-based method of binning seeks to optimally reduce variable count while retaining spectral information by applying a Gaussian weighting function [57]. Other adaptive binning methods rely on a recursive algorithm [56], undecimated wavelet transforms [58] or the optimization of an objective function using a dynamic programming strategy [59] to identify bin edges. Regardless of the approach, adaptive binning performs significantly better than uniform binning [59]. Alternatively, full-resolution spectral signals may be computationally aligned within a dataset to remove chemical shift variability, retaining the possibility of avoiding binning and performing multivariate analysis with less loss of spectral information [60-65]. Spectral alignment has been accomplished using a variety of approaches that includes fuzzy warping, genetic algorithms, a generalized fuzzy Hough transform approach, a reduced set mapping (PARS) algorithm, or a recursive segment-wise peak alignment. Importantly, spectral alignment was shown to improve upon the results obtained using adaptive binning [65]. Sample acidification has also been used prior to data collection to force peaks into alignment [66]. Finally, it has been demonstrated that OPLS-DA more



effectively copes with chemical shift variation in full-resolution  $^1\text{H}$  NMR datasets [67] without requiring binning or alignment steps.

A similar alignment problem arises in the retention times of chromatograms used in GC-MS and LC-MS metabolomics experiments, where shifts in observed metabolite retention times between samples can obscure true relationships in model loadings [68]. The use of correlation optimized warping (COW), a specialized form of dynamic time warping (DTW), has recently found success in bringing peaks in chromatographic datasets into alignment by means of a dynamic programming algorithm [69, 70]. Methods of automated optimal parameter selection for COW have also been introduced, reducing the amount of operator intervention required for aligning large datasets [71]. Maven [72], MetaboAnalyst [73], MZmine [74] and PolyAlign [75] are just a few examples of some popular alignment software programs and metabolomics work-flow packages that are available. Some recent alternatives to COW approach to peak alignment include model-base [76], density maximization [77], fuzzy clustering [78] or maximum-likelihood [79].

### Data normalization

To account for variable dilution factors of metabolic fingerprinting samples arising from variations in the number of cells, biofluid volume or tissue size, each observation row in  $\mathbf{X}$  may be normalized to ensure that all observations are directly comparable. Normalization may be accomplished internally by computational means using internal standards (e.g. TMS in NMR) [80, 81] or externally via measurements of cell culture optical density or protein content. The simplest form of internal scaling, called constant-sum normalization, is where each spectrum is normalized such that its integral is 1. While this accounts for variable dilutions each sample may possess, it can mask truly biologically relevant changes and obscure interpretation of loadings [80].

### Data scaling

While the discussed forms of multivariate analysis are defined based on the covariance eigenstructure of  $\mathbf{X}$  and  $\mathbf{Y}$ , practical considerations motivate the use of variable scaling prior to analysis. From an intuitive standpoint, a linear combination of observations from different instrumental sources –  $^1\text{H}$  NMR and MS, for example – has no physical meaning. However, even when all variables bear identical units, highly disparate intensities and variances between variables will force most forms of multivariate analysis to focus on a small set of intense signals [44]. For these reasons, variables may be autoscaled to have zero mean and unit variance through a  $z$ -scoring operation [80] that results in PCA and PLS examining correlations, rather than covariances, in  $\mathbf{X}$  and  $\mathbf{Y}$ . Myriad other forms of scaling exist (Table 1), each of which enhance different features in the data and carry different disadvantages, which may suit every metabolic profiling experiment differently [82]. Figure 3 shows the results of applying unit variance autoscaling to a set of simulated two-peak NMR spectra.

### Noise and baseline removal

A principal disadvantage of data scaling is its tendency to amplify instrumental noise, to which PCA and PLS have been shown to be sensitive [52, 83]. Methods of scaling based on Maximum Likelihood PCA (MLPCA) [84] have been used to estimate and remove

instrumental errors prior to multivariate analysis [85]. More simply, domain knowledge may be used to preselect variables based on experimental relevance or noise criteria for the removal of signal-free baseline noise from acquired spectra or the selection of more narrow spectral regions [86].

### Variable selection

Due to the expense of sampling and data collection in metabolomics experiments, a tendency exists in metabolic fingerprinting studies to retain all collected variables for multivariate analysis [86]. Unfortunately, this exacerbates the aforementioned collinearity problem and increases the likelihood of finding spurious correlations in data, leading to a greater chance of inferring incorrect biological conclusions [46, 51]. While it is not typically performed during data exploration, variable selection may be used conservatively in concert with domain knowledge to select only biologically meaningful regions of datasets for classification or dimensionality reduction.  $^1\text{H}$  NMR datasets, for instance, may contain highly varying signals from solvents, buffers and chemical shift reference compounds, as well as large signal-free noise regions. Both of these features may obscure biologically relevant variation and are good candidates for variable selection/removal. Structured noise (baseline issues, contaminants) negatively affects the correspondence between scores and loadings and hinders the correct interpretation of PLS results [87]. OPLS can separate out this structured noise, but often at the expense of an overly complex model [88]. There are significantly more variables ( $K$ ) than observations ( $N$ ) in a typical metabolomics dataset, so removing irrelevant variables is beneficial to the multivariate analysis. A more exhaustive variable selection approach applies a pretreatment based on orthogonal projections [89] or a recursive algorithm [90-92], support vector machine, genetic algorithm or random forest, to select for variables or spectral features primarily contributing to class separation. This is particularly pertinent to MS metabolomics data that may contain a very large number of variables, of which only a small percentage is relevant. Importantly, either the complete absence of variable selection or an overly aggressive variable selection may lead to inadequate separation or over-fitting of the dataset, respectively [92, 93].

### Interpretation

Interpretation of multivariate analysis results of metabolic fingerprinting data for the purposes of inferring biological importance must be done with care, bearing in mind the nature and goal of the algorithm used. Scatter plots of scores and loadings are no exception, particularly since different axis scaling can produce misleading results [86, 94]. As an illustration, an observed difference in a scores plot comparing spectral data obtained from healthy and ill patients may infer the existence of potential disease biomarkers. Thus, it is imperative to verify that this variation is due to an underlying biological source instead of artifacts induced by the algorithm, sample handling or data processing.

### Scores

Scores produced by PCA and PLS are the observation rows of  $X$  projected onto a hyperplane within the data that describes the covariances of  $X$ , or the covariances between  $X$  and  $Y$ , respectively. In a nutshell, scores are good 'summaries' of the observations [35]. Because

fewer predictive components are required to yield discrimination in OPLS-DA, two-class scores plots are commonly built from one predictive component and one orthogonal component. For PCA, class separations in scores are exposed only when within-class variation is less than between-class variation. Because of this, misleading class separation in a PCA scores plot is not a function of the algorithm, but occurs from sample preparation problems [95], experimental bias [96], or inappropriate data preprocessing [82]. Contrary to PCA, PLS and OPLS aggressively over-fit models to the data, almost always yielding scores in which classes are separated [88]. As a result, PLS and OPLS can generate excellent class separation even with random data (Figure 4) [86]. Thus, extreme care must be taken not to infer model reliability from the existence of class separations in PLS or OPLS scores. In effect, the use of PLS or OPLS models necessitates validation [97].

For PCA and validated PLS scores, quantitative measures must be applied to reliably infer significant separations between classes within a scores plot [98]. Simply, a visual inspection of the clustering pattern or class separation in a scores plot is not typically sufficient to infer statistical relevance. Methods using cluster overlap metrics [99], statistical distances [98], and hierarchical clustering [100, 101] have been successfully used to quantify separations in scores plots. Also, class membership may be inferred from 95% confidence ellipses calculated from scores [101].

## Loadings

Loadings from PCA and (O)PLS are the directions of the hyperplane mentioned above with respect to the original  $X$  variables, and function as good 'summaries' of the variables' influence on the model. Due to the complementary nature of scores and loadings as explanations of the rows and columns of  $X$ , respectively, the two may be used in concert. Variables whose loadings are co-located away from the origin in a loadings plot may be inferred to be correlated. Moreover, variables with loadings in a given position in a loadings plot contribute heavily to observations whose scores are found in a similar position in a scores plot. This requires proper normalization such that the scores and loadings are on the same scale, where the loadings closest to the scores are expected to have the highest contribution to class separation. The ease of interpretation of loadings is directly affected by the number of variables and the scaling method used, if any [82]. As indicated by Table 1, scaling protocols emphasize different spectral features which will then perturb the influence of a particular variable on the model. In turn, the magnitude of the corresponding loadings will be proportionally affected. As an example, Pareto scaling is commonly used to reduce the influence of intense peaks while emphasizing weaker peaks that may have more biological relevance. The corresponding loadings of intense peaks will be reduced and loadings from weak peaks will be increased due to Pareto scaling.

Loadings may also be examined on a per-component basis as a line plot, with the loading value plotted as dependent upon the spectral variables (ppm,  $m/z$ ,  $\nu$ ). This is especially valuable when full-resolution spectra are used as data. In this form, the loadings of each model component may be viewed as a spectrum or pseudo-spectrum, with large positive or negative excursions of a variable's loading corresponding to a large positive or negative correlation with class structure, respectively. With full-resolution spectra and OPLS-DA

models, this method of interpreting loadings is highly useful for identifying metabolites contributing to class differences [67, 102]. Pareto scaling has an added advantage in this context, as it better preserves spectral lineshapes in loading pseudo-spectra. Of course, large loadings corresponding to irrelevant spectral regions such as noise, artifacts, buffers, or solvent peaks, raise serious concerns about the biological relevance of the model.

## Weights

The weights produced in  $\mathbf{A}$  by multivariate analysis are the relative degrees of influence that each observed variable in  $\mathbf{X}$  has on each of the latent structures in the model, and are used to transform new observation vectors from later measurements into scores space for the purposes of class prediction. A common misconception is misrepresenting loadings as weights for the purposes of identifying variable or metabolite contribution to class separation.

## Validation

PLS and OPLS have an innate tendency to over-fit models to data, even identifying excellent class separation in completely random variables as demonstrated in Figure 4 [88]. For PLS and OPLS, validation is a critical step in ensuring model reliability. Truly honest model validation requires partitioning the data into a training set used to build a model and a validation set used to assess predictive ability of the model, where the validation set is in no way used to generate the trained model [103, 104]. Few practitioners have adopted this method of validation because of the low sample count in metabolic fingerprinting experiments and the costly nature of sample preparation and data acquisition. Instead, internal cross-validation is routinely employed, where the leave-one-out method is a common choice [105]. However, it has been demonstrated that leave-one-out internal cross-validation should be abandoned [106-108] in favor of the more consistent leave- $n$ -out method.

In the leave- $n$ -out method, the data is partitioned into  $\binom{N}{n}$  subsets, where each of the subsets is then used as a validation set [109, 110]. As true leave- $n$ -out cross-validation is computationally inefficient, Monte Carlo cross-validation may be utilized to rapidly estimate model prediction ability [111, 112]. The quality assessment ( $Q^2$ ) statistic is typically reported as a result of cross-validation and provides a qualitative measure of consistency between the predicted and original data. Even still,  $Q^2$  has no standard of comparison or critical value for inferring significance, aside from its theoretical maximum of 1 or an empirically inferred acceptable value of 0.4 for a biological model [88]. Unfortunately, an invalid or irrelevant model is still capable of producing a large  $Q^2$  value, since consistent cross-validation requires a systematic deletion of large portions of its dataset during training. One solution recently demonstrated for metabolomics combines random permutation of class labels, which requires no deletion of data, with internal leave- $n$ -out cross-validation [88]. The approach produces a distribution of  $Q^2$  values suitable for testing the null hypothesis for a model's  $Q^2$ . In essence, a reliable model should yield a significantly larger  $Q^2$  value compared to  $Q^2$  values generated from random models using the same data set. The technique is also valid for testing null hypotheses for the area under Receiver Operating

Characteristic (ROC) curves (AUROC) statistic and misclassification count. Another method, the CV-ANOVA, uses the cross-validated predictive residuals of a model as a basis for hypothesis testing [97].

Also, while they are not strictly a cross validation measure, the  $R^2$  values of a given model may be used to assess its degree of fit to the data [35, 44]. PCA decompositions will return only  $R^2X$ , the degree to which the principal components describe the observation data, and PLS decompositions will return both  $R^2X$  and  $R^2Y$ . Due to its division of  $X$  into  $X^*$  and  $X^{\circ}$ , OPLS splits  $R^2X$  into  $R^2X_p$  and  $R^2X_o$ , the explained sum of squares of the  $Y$ -predictive and  $Y$ -uncorrelated components of  $X$ , respectively. Highly disparate  $R^2$  and  $Q^2$  values (i.e.  $R^2$ ,  $Q^2$ ) are an indicator of possible model over-fitting in supervised analyses.

## Applications

### Raman and NMR Fingerprinting of Rat Urine

The application of Raman spectroscopy to the study of metabolite fingerprints has occurred only relatively recently compared with the more mature NMR and MS techniques [31]. A comparative analysis demonstrates Raman spectroscopy offers complementary spectral information to NMR [40]. In the study, three groups of rats were orally fed different triazole fungicides, and a fourth group was fed only the drug carrier vehicle as a control. After five days of exposure, urine was collected from the rats and subjected to both  $^1\text{H}$  NMR and Raman spectroscopy. NMR spectra were acquired on a Varian Inova 800 spectrometer with a spectral width of 12.5 ppm over 64k data points using a standard 1D pre-saturation pulse sequence. Peaks corresponding to the solvent, urea and carrier vehicle were removed from the spectra, which were then truncated to 0.5 – 9.5 ppm extents and integrated into 0.04 ppm-wide bins. The NMR bins were then mean-centered and Pareto scaled [82] prior to PCA.

While collection and PCA of Raman spectra was performed in similar fashion to the NMR data, several marked differences exist. First, samples for Raman analysis were subjected to ultrafiltration to remove fluorescent biomacromolecules having molecular weights greater than 500 Da. While the filtration step reduced biologically irrelevant chemical noise in the collected spectra, the authors noted that the tricarboxylates citrate, *trans*-aconitinate, and oxoglutarate were significantly removed in the process. Raman spectra were then collected with 785 nm laser excitation at  $\sim 5\text{ cm}^{-1}$  resolution between  $\sim 3280 - 95\text{ cm}^{-1}$ . Unlike the collected NMR spectra, Raman peaks showed no significant pH-dependent variation, permitting the full spectral resolution to be used in PCA without binning or alignment. Spectra of urea and sodium azide were subtracted from each spectrum, which were then truncated to  $1705 - 467\text{ cm}^{-1}$ , mean-subtracted, normalized to constant AUC and submitted to PCA and PLS-DA.

Figure 5 shows a comparison of the PCA scores produced by the collected NMR and Raman datasets. From the scores, it can be seen that the within-class variation of the Raman spectra is noticeably lower than that of the NMR spectra, effectively showing a better separation for the collected samples. However, due to the low number of spectra collected for each experimental class, it is difficult to judge class separations on a statistical basis. The authors

note that PCA captured a greater percentage variance of the Raman spectra than the NMR spectra, suggesting better performance. This use of captured variance is incorrect, however, as captured variance is a relative measure that only describes model performance for any given dataset and not between different datasets.

Finally, two-class PLS-DA was used to find loadings in the Raman spectra that discriminated between each fungicide treatment and the control. Significant changes in the loadings were found to coincide with transitions of the metabolites allantoin, creatine, alanine, taurine, acetate and hippurate. However, no measures of validation were provided to lend statistical credence to the observed metabolite changes. The class distinction present in the PCA scores plot does suggest the same class separation in the PLS-DA is likely correct. But, the PLS-DA model could still be over-fitted to the data, leading to an invalid model and incorrect loadings. As a result, the identified metabolites could be biologically irrelevant. This is not necessarily true, but it is plausible outcome in the absence of a validated PLS-DA model. Nevertheless, the study does provide an illustrative proof-of-principle for Raman spectroscopy-based metabolic fingerprinting which, with further tuning, promises to be a useful instrumental platform for metabolomics.

### Discrimination of French Labeled Brandy

While the metabolite profiles of many brandies were previously known, marker metabolites that could be used to discriminate between different types of brandy were not identified. Such metabolites could be used in determination of the origin and authenticity of French labeled brandies. To that end, gas chromatography mass spectrometry (GC-MS) analyses of Cognac, Armagnac, Calvados and Mirabelle were analyzed and subjected to PLS-DA [113]. Ethyl undecanoate and 4-methylpentan-2-ol were added to the brandy samples for use as internal standards, and two liquid-liquid extractions were used to isolate the volatile organic molecules from the samples.

Peaks in the collected GC-MS spectra having a signal-to-noise greater than 10 were linked with compounds using database searches based on electron impact spectra and retention indices; the resulting intensities of all compounds were then normalized to the internal standards. The data matrix was then generated using the calculated relative compound concentrations, which were mean-centered and autoscaled to unit variance prior to PLS-DA. This particular study highlights the flexibility of multivariate analysis methods to accept any type of variable, not only raw spectral information, for modeling purposes in metabolomics.

Figure 6 shows the variable loadings from PLS-DA plotted for the two discriminatory components found in the GC-MS dataset. The authors understandably described the loadings as weights in the manuscript, a confusing description exacerbated by the SIMCA (UMETRICS) nomenclature for PLS loadings ( $w^*C[n]$ ). Unfortunately, the SIMCA loadings nomenclature appears startlingly similar to the PLS regression coefficients [35], the product of  $X$ -weights and  $Y$ -weights, and not the loadings. However, in PLS loading plots of this type, the  $X$ -weights ( $w^*$ ) and  $Y$ -weights ( $C$ ) are simply plotted together – not multiplied – in order to expose the correlation structure between  $X$  and  $Y$ . The loadings for each type of brandy in scores space were printed on the loadings plot to aid in identifying compounds that contribute most to the discrimination between each of the beverage types.



Importantly, loadings must be non-zero along any principal component axis to have any contribution to the model.

Each loading is correlated to a particular  $X$ -variable, in this case the molecular-weight of a particular metabolite. Thus, the loadings strongly correlated with scores for each type of brandy identify metabolites that may uniquely describe or characterize that particular brandy. While the volatile compound identification and quantification procedure resulted in a great wealth of useful information, no validation statistics were provided to justify the discriminatory compounds selected from the PLS-DA loadings. Again, the lack of appropriate validation is a common problem among the metabolomics community.

### Correlations of Human Gut Microbiome with Urine Metabolites

Studies have shown that the microbiome – the sum total of all microbial organisms – of the human gastrointestinal tract has a great impact on individual metabolite profiles, even when genetic variations are minimized [114]. Changes in the symbiotic gut microbes correlate with phenotypic variations observed between gender and across ethnicities, and are implicated in many forms of human pathology. Recent work based on the gut microbiomes and urine metabolic fingerprints of Chinese family members has shed light onto correlations between gut flora and phenotype [45].

In the study by Li *et al.*, selected portions of the bacterial genomes of family members' gut microbiota were subjected to denaturing gradient gel electrophoresis (DGGE), and urine samples were also collected from each family member and analyzed by  $^1\text{H}$  NMR spectroscopy. OPLS-DA was used to identify gender-predictive components of the DGGE gels and NMR spectra. The  $Q^2$  value of each variable obtained by five-fold internal cross-validation was used to identify statistically reliable loadings in the OPLS-DA models. Species of *Clostridia*, *Bacteroidetes* and *Proteobacteria* were found to be predictive of gender based on DGGE gels, and 3-aminoisobutyrate and creatine were found to predict gender from the NMR spectra.

A cross-correlation analysis was also performed to model the DGGE gel bands using NMR spectral data, and *vice versa*, using OPLS regression. Again, five-fold internal cross-validation was performed to ensure model reliability, and the predictions of NMR peaks and DGGE bands made by the model were color-coded according to  $Q^2$  to facilitate rapid identification of significant correlations. A correlation matrix was also constructed to show peaks in the collected NMR spectra that co-varied with bands in the DGGE gel. Figure 7 summarizes the results of the cross-correlation analysis. This study highlights a powerful use of OPLS, both in discrimination and regression applications, as well as the use of cross-validation statistics.

### Analysis of Bacterial Metabolic Signaling of Stress Response

It has been shown that the stress response of prokaryotic organisms contains a metabolic sensing component, centered around the tricarboxylic acid (TCA) cycle and sensed by catabolite control protein A (CcpA), that effects downstream signaling networks involved in virulence factor presentation and biofilm formation [115]. Metabolic fingerprinting using  $^1\text{H}$



NMR spectroscopy was conducted to further examine the effects of external biofilm-inducing perturbations on the metabolome of *Staphylococcus epidermidis* [116]. Metabolite mixtures were collected from wild-type cells, as well as cells exposed to sodium chloride, glucose, tetracycline, ethanol, iron-depleted media, and an aconitase deletion mutation.

PCA analysis of the NMR spectra revealed that the sodium chloride-treated cells grouped with the wild-type in scores space. All other observations on treated cells group together in scores space except for glucose treatment, which clustered separately from all observations. The separations between classes in the PCA scores were used to define two classes for a subsequent OPLS-DA analysis, with wild-type and salt-treated cells discriminated from all other observations. Figure 8 shows the OPLS scores plot and dendrogram resulting from decomposition into one  $Y$ -predictive component and three  $Y$ -uncorrelated components. In the OPLS model, the explained sum of squares for  $X$  and  $Y$  were found to be 0.637 and 0.966, respectively. It is important to note that the reported  $R^2X$  of 0.637 includes  $Y$ -uncorrelated variation, and is therefore not a measure of modeled *predictive* variation. Leave- $n$ -out internal cross-validation resulted in a  $Q^2$  value of 0.941, an acceptable value in light of the models  $R^2Y$ , but by no means conclusive. While it was not performed for the publication, a subsequent validation using CV-ANOVA provided a  $p$ -value of 0.0 – to within machine precision [117] – for the OPLS model.

### Future Directions

Multivariate analysis of metabolic fingerprinting datasets is performed most often with the linear projection-based methods of PCA, PLS and OPLS, but these are by no means the only tools available. Hierarchical clustering analysis (HCA) and nearest-neighbor clustering may be applied to multivariate spectral data to reveal differences between classes without supervision. Support-vector machine (SVM) methods [118] have been applied to human urine metabolomics NMR [119], NIR and UV datasets [120] with enhanced predictive power over PLS-DA. Artificial neural networks (ANN) have also been used in combination with PCA for plant metabolic profiling and fingerprinting [121, 122]. In contrast to pure PCA and PLS, which model linear relationships, both SVM and ANN algorithms admit the use of a kernel function to allow for modeling of non-linear relationships between  $X$  and  $Y$ . However, none of these methods provide quite the interpretative simplicity of projective ‘latent-space’ methods such as PCA and PLS. The metabolomics community is accustomed to drawing conclusions from PCA and PLS results, but these new methods with their unfamiliar analysis formats require further acclimation.

Finally, the majority of multivariate analysis techniques used in metabolic fingerprinting are designed for ‘snapshot’ datasets, where the state of a system is observed at one or two highly distinct time points. However, as instrumental methods improve to accommodate measurement of highly time-resolved metabolite concentration changes, methods of multivariate analysis must be developed to cope with the new information [123]. Multi-way data analysis methods such as Parallel Factor Analysis (PARAFAC [124]), consensus PCA (CPCA) and multi-block PLS are all suited to particular types of multi-way datasets [125]. Somewhat similar in form to time-resolved metabolomic datasets are those produced by the fusion of data from orthogonal or complementary instrumentation. For example,  $^1\text{H}$  NMR

and LC-MS data matrices have been combined by multiple means to achieve improved PCA and PLS models [126]. GC-MS and LC-MS datasets [127], as well as near-IR and mid-IR spectral datasets [128] have been similarly fused for the purposes of multivariate analysis.

### Concluding Remarks

Techniques such as PCA and PLS provide an essential platform for rapid interpretation of information-rich spectral datasets for inferring biological conclusions. Through proper application of preprocessing transformations, optimal choice of analysis algorithms, and judicious application of validation metrics, MVA can lend a powerful hand in the biological understanding and exploration of complex, multiparametric metabolic systems. Unfortunately, misunderstandings and the misuse of MVA can lead to misleading or erroneous biological inferences. The few examples highlighted in this review are just a sampling of the large number of metabolomics studies with similar problems. Additionally, metabolomics has many data challenges left to be solved, and machine learning chemometrics methods have much to offer metabolomics.

### References

1. Lindon JC, Nicholson JK, Holmes E, Everett JR. Metabonomics: Metabolic processes studied by NMR spectroscopy of biofluids. *Concept Magnetic Res.* 2000; 12(5):289–320.
2. Kell DB. Metabolomics and systems biology: making sense of the soup. *Curr Opin Microbiol.* 2004; 7(3):296–307. [PubMed: 15196499]
3. Trethewey RN. Gene discovery via metabolic profiling. *Curr Opin Biotechnol.* 2001; 12(2):135–138. [PubMed: 11287226]
4. Weckwerth W. Metabolomics in systems biology. *Annu Rev Plant Biol.* 2003; 54:669–689. [PubMed: 14503007]
5. Navon G, Burrows H, Cohen JS. Differences in metabolite levels upon differentiation of intact neuroblastoma \* glioma cells observed by proton NMR spectroscopy. *FEBS Lett.* 1983; 162(2): 320–323. [PubMed: 6313424]
6. Pfeuffer J, Tkac I, Provencher SW, Gruetter R. Toward an in Vivo Neurochemical Profile: Quantification of 18 Metabolites in Short-Echo-Time 1H NMR Spectra of the Rat Brain. *J Magn Reson.* 1999; 141(1):104–120. [PubMed: 10527748]
7. ter Kuile BH, Westerhoff HV. Transcriptome meets metabolome: hierarchical and metabolic regulation of the glycolytic pathway. *FEBS Lett.* 2001; 500(3):169–171. [PubMed: 11445079]
8. Gebregiworgis T, Powers R. Application of NMR Metabolomics to Search for Human Disease Biomarkers. *Comb Chem High Throughput Screening.* 2012; 15(8):595–610.
9. Vinayavekhin N, Homan EA, Saghatelian A. Exploring Disease through Metabolomics. *ACS Chem Biol.* 2010; 5(1):91–103. [PubMed: 20020774]
10. Powers R. NMR metabolomics and drug discovery. *Magn Reson Chem.* 2009; 47:S2–S11. [PubMed: 19504464]
11. Wilcoxon KM, Uehara T, Myint KT, Sato Y, Oda Y. Practical metabolomics in drug discovery. *Expert Opin Drug Discovery.* 2010; 5(3):249–263.
12. Hall RD. Plant metabolomics in a nutshell: potential and future challenges. *Annu Plant Rev.* 2011; 43:1–24. *Biology of Plant Metabolomics.*
13. Zhang B, Powers R. Using NMR-based metabolomics to study the regulation of biofilm formation. *Future Med Chem.* 2012; 4(10):1273–1306. [PubMed: 22800371]
14. Tang J. Microbial metabolomics. *Curr Genomics.* 2011; 12(6):391–403. [PubMed: 22379393]
15. McNiven EMS, German JB, Slupsky CM. Analytical metabolomics: nutritional opportunities for personalized health. *J Nutr Biochem.* 2011; 22(11):995–1002. [PubMed: 21999844]

16. Bundy JG, Davey MP, Viant MR. Environmental metabolomics: a critical review and future perspectives. *Metabolomics*. 2009; 5(1):3–21.
17. Baker M. Metabolomics: From small molecules to big ideas. *Nat Methods*. 2011; 8(2):117–121.
18. Dunn WB, Ellis DI. Metabolomics: Current analytical platforms and methodologies. *Trac-Trends in Anal Chem*. 2005; 24(4):285–294.
19. Pearson H. Meet the human metabolome. *Nature*. 2007; 446(7131):8. [PubMed: 17330009]
20. Wishart DS, Tzur D, Knox C, Eisner R, Guo AC, Young N, Cheng D, Jewell K, Arndt D, Sawhney S, Fung C, Nikolai L, Lewis M, Coutouly MA, Forsythe I, Tang P, Shrivastava S, Jeroncic K, Stothard P, Amegbey G, Block D, Hau DD, Wagner J, Miniaci J, Clements M, Gebremedhin M, Guo N, Zhang Y, Duggan GE, MacInnis GG, Weljie AM, Dowlatabadi R, Bamforth F, Clive D, Greiner R, Li L, Marrie T, Sykes BD, Vogel HJ, Querengesser L. HMDB: the Human Metabolome Database. *Nucleic Acids Res*. 2007; 35(Database Iss):D521–D526. [PubMed: 17202168]
21. Cui Q, Lewis IA, Hegeman AD, Anderson ME, Li J, Schulte CF, Westler WM, Eghbalian HR, Sussman MR, Markley JL. Metabolite identification via the Madison Metabolomics Consortium Database. *Nat Biotechnol*. 2008; 26(2):162–164. [PubMed: 18259166]
22. Kind T, Wohlgemuth G, Lee DY, Lu Y, Palazoglu M, Shahbaz S, Fiehn O. FiehnLib: Mass Spectral and Retention Index Libraries for Metabolomics Based on Quadrupole and Time-of-Flight Gas Chromatography/Mass Spectrometry. *Anal Chem*. 2009; 81(24):10038–10048. [PubMed: 19928838]
23. Dettmer K, Aronov PA, Hammock BD. Mass spectrometry-based metabolomics. *Mass Spectrom Rev*. 2007; 26(1):51–78. [PubMed: 16921475]
24. Viswanadhan VN, Rajesh H, Balaji VN. Atom Type Preferences, Structural Diversity, and Property Profiles of Known Drugs, Leads, and Nondrugs: A Comparative Assessment. *ACS Comb Sci*. 2011; 13(3):327–336. [PubMed: 21480669]
25. Rubakhin SS, Romanova EV, Nemes P, Sweedler JV. Profiling metabolites and peptides in single cells. *Nat Methods*. 2011; 8(4):S20–S29. [PubMed: 21451513]
26. Aoki-Kinoshita KF. Overview of KEGG applications to omics-related research. *J Pestic Sci (Tokyo, Jpn)*. 2006; 31(3):296–299.
27. Alvarez-Sanchez B, Priego-Capote F, Luque dCMD. Metabolomics analysis I. Selection of biological samples and practical aspects preceding sample preparation. *TrAC, Trends Anal Chem*. 2010; 29(2):111–119.
28. Alvarez-Sanchez B, Priego-Capote F, Luque dCMD. Metabolomics analysis II. Preparation of biological samples prior to detection. *TrAC, Trends Anal Chem*. 2010; 29(2):120–127.
29. Tyagi S, Raghvendra, Singh U, Kalra T, Munjal K. Applications of Metabolomics - a systematic study of the unique chemical fingerprints: an overview. *Int J Pharm Sci Rev Res*. 2010; 3(1):83–86.
30. Han J, Datla R, Chan S, Borchers CH. Mass spectrometry-based technologies for high-throughput metabolomics. *Bioanalysis*. 2009; 1(9):1665–1684. [PubMed: 21083110]
31. Ellis DI, Goodacre R. Metabolic fingerprinting in disease diagnosis: biomedical applications of infrared and Raman spectroscopy. *Analyst*. 2006; 131(8):875–885. [PubMed: 17028718]
32. Pearson K. On Lines and Planes of Closest Fit to Systems of Points in Space. *Philos Mag*. 1901; 2(6):14.
33. Hotelling H. Analysis of a complex of statistical variables into principal components. *J Educ Psychol*. 1933; 24(7):22.
34. Wold, S.; Johansson, E.; Cocchi, M. PLS. In: Kubinyi, H., editor. 3D-QSAR in Drug Design: Theory, Methods and Applications. ESCOM Science; Ledien: 1993. p. 523-550.
35. Wold S, Sjostrom M, Eriksson L. PLS-regression: a basic tool of chemometrics. *Chemometr Intell Lab*. 2001; 58(2):109–130.
36. Beckonert O, Keun HC, Ebbels TMD, Bundy J, Holmes E, Lindon JC, Nicholson JK. Metabolic profiling, metabolomic and metabonomic procedures for NMR spectroscopy of urine, plasma, serum and tissue extracts. *Nat Protocols*. 2007; 2(11):2692–2703.
37. Koh P, Chan E, Mal M, Eu K, Blackshall A, Keun H. Metabolic Profiling of Human Colorectal Cancer Using High-Resolution Magic Angle Spinning Nuclear Magnetic Resonance (Hr-Mas

- Nmr) Spectroscopy and Gas Chromatography Mass Spectrometry (Gc/Ms). *Dis Colon Rectum*. 2009; 52(4):769–769.
38. Goodacre R, York EV, Heald JK, Scott IM. Chemometric discrimination of unfractionated plant extracts analyzed by electrospray mass spectrometry. *Phytochemistry*. 2003; 62(6):859–863. [PubMed: 12590113]
  39. Wu HF, Southam AD, Hines A, Viant MR. High-throughput tissue extraction protocol for NMR- and MS-based metabolomics. *Anal Biochem*. 2008; 372(2):204–212. [PubMed: 17963684]
  40. Cherney DP, Ekman DR, Dix DJ, Collette TW. Raman spectroscopy-based metabolomics for differentiating exposures to triazole fungicides using rat urine. *Anal Chem*. 2007; 79(19):7324–7332. [PubMed: 17718537]
  41. Garcia-Perez I, Vallejo M, Garcia A, Legido-Quigley C, Barbas C. Metabolic fingerprinting with capillary electrophoresis. *J Chromatogr A*. 2008; 1204(2):130–139. [PubMed: 18656201]
  42. Ramautar R, Demirci A, de Jong GJ. Capillary electrophoresis in metabolomics. *Trac-Trends in Anal Chem*. 2006; 25(5):455–466.
  43. Bylesjo M, Rantalainen M, Cloarec O, Nicholson JK, Holmes E, Trygg J. OPLS discriminant analysis: combining the strengths of PLS-DA and SIMCA classification. *J Chemom*. 2006; 20(8-10):341–351.
  44. Jolliffe, IT. *Principal Component Analysis*. 2. Springer; 2002.
  45. Li M, Wang BH, Zhang MH, Rantalainen M, Wang SY, Zhou HK, Zhang Y, Shen J, Pang XY, Zhang ML, Wei H, Chen Y, Lu HF, Zuo J, Su MM, Qiu YP, Jia W, Xiao CN, Smith LM, Yang SL, Holmes E, Tang HR, Zhao GP, Nicholson JK, Li LJ, Zhao LP. Symbiotic gut microbes modulate human metabolic phenotypes. *Proc Natl Acad Sci U S A*. 2008; 105(6):2117–2122. [PubMed: 18252821]
  46. Johnstone IM, Titterton DM. Statistical challenges of high-dimensional data. *Phil Trans R Soc A*. 2009; 367(1906):4237–4253. [PubMed: 19805443]
  47. Barker M, Rayens W. Partial least squares for discrimination. *J Chemom*. 2003; 17(3):166–173.
  48. Rannar S, Lindgren F, Geladi P, Wold S. A PLS Kernel Algorithm for Data Sets with Many Variables and Fewer Objects .1. Theory and Algorithm. *J Chemom*. 1994; 8(2):111–125.
  49. Wold S, Antti H, Lindgren F, Ohman J. Orthogonal signal correction of near-infrared spectra. *Chemometr Intell Lab*. 1998; 44(1-2):175–185.
  50. Sjoblom J, Svensson O, Josefson M, Kullberg H, Wold S. An evaluation of orthogonal signal correction applied to calibration transfer of near infrared spectra. *Chemometr Intell Lab*. 1998; 44(1-2):229–244.
  51. Hoskuldsson A. Variable and subset selection in PLS regression. *Chemometr Intell Lab*. 2001; 55(1-2):23–38.
  52. Trygg J, Wold S. Orthogonal projections to latent structures (O-PLS). *J Chemom*. 2002; 16(3): 119–128.
  53. Tapp HS, Kemsley EK. Notes on the practical utility of OPLS. *Trac-Trends in Anal Chem*. 2009; 28(11):1322–1327.
  54. Lindon JC, Nicholson JK, Holmes E, Keun HC, Craig A, Pearce JTM, Bruce SJ, Hardy N, Sansone SA, Antti H, Jonsson P, Daykin C, Navarange M, Beger RD, Verheij ER, Amberg A, Baunsgaard D, Cantor GH, Lehman-McKeeman L, Earll M, Wold S, Johansson E, Haselden JN, Kramer K, Thomas C, Lindberg J, Schuppe-Koistinen I, Wilson ID, Reily MD, Robertson DG, Senn H, Krotzky A, Kochhar S, Powell J, van der Ouderaa F, Plumb R, Schaefer H, Spraul M, worki SMRS. Summary recommendations for standardization and reporting of metabolic analyses. *Nat Biotechnol*. 2005; 23(7):833–838. [PubMed: 16003371]
  55. Goodacre R, Broadhurst D, Smilde AK, Kristal BS, Baker JD, Beger R, Bessant C, Connor S, Calmani G, Craig A, Ebbels T, Kell DB, Manetti C, Newton J, Paternostro G, Somorjai R, Sjoström M, Trygg J, Wulfert F. Proposed minimum reporting standards for data analysis in metabolomics. *Metabolomics*. 2007; 3(3):231–241.
  56. De Meyer T, Sinnaeve D, Van Gasse B, Tsioporkova E, Rietzschel ER, De Buyzere ML, Gillebert TC, Bekaert S, Martins JC, Van Criekinge W. NMR-Based Characterization of Metabolic Alterations in Hypertension Using an Adaptive, Intelligent Binning Algorithm. *Anal Chem*. 2008; 80(10):3783–3790. [PubMed: 18419139]

57. Anderson PE, Reo NV, DelRaso NJ, Doom TE, Raymer ML. Gaussian binning: a new kernel-based method for processing NMR spectroscopic data for metabolomics. *Metabolomics*. 2008; 4(3):261–272.
58. Davis RA, Charlton AJ, Godward J, Jones SA, Harrison M, Wilson JC. Adaptive binning: An improved binning method for metabolomics data using the undecimated wavelet transform. *Chemom Intell Lab Syst*. 2007; 85(1):144–154.
59. Anderson PE, Mahle DA, Doom TE, Reo NV, Del RNJ, Raymer ML. Dynamic adaptive binning: an improved quantification technique for NMR spectroscopic data. *Metabolomics*. 2011; 7(2): 179–190.
60. Vu TT, Valkenburg D, Smets K, Verwaest KA, Dommissie R, Lemiere F, Verschoren A, Goethals B, Laukens K. An integrated workflow for robust alignment and simplified quantitative analysis of NMR spectrometry data. *BMC Bioinformatics*. 2011; 12
61. Wu W, Daszykowski M, Walczak B, Sweatman BC, Connor SC, Haseldeo JN, Crowther DJ, Gill RW, Lutz MW. Peak alignment of urine NMR spectra using fuzzy warping. *J Chem Inf Model*. 2006; 46(2):863–875. [PubMed: 16563018]
62. Zhou W, Seoung Bum K. Automatic Alignment of High-Resolution NMR Spectra Using a Bayesian Estimation Approach. *Proceedings of the 18th International Conference on Pattern Recognition*. 2006; 4:667–670.
63. Forshed J, Schuppe-Koistinen I, Jacobsson SP. Peak alignment of NMR signals by means of a genetic algorithm. *Anal Chim Acta*. 2003; 487(2):189–199.
64. Veselkov KA, Lindon JC, Ebbels TMD, Crockford D, Volynkin VV, Holmes E, Davies DB, Nicholson JK. Recursive Segment-Wise Peak Alignment of Biological 1H NMR Spectra for Improved Metabolic Biomarker Recovery. *Anal Chem*. 2009; 81(1):56–66. [PubMed: 19049366]
65. Csenki L, Alm E, Torgrip RJO, Aaberg KM, Nord LI, Schuppe-Koistinen I, Lindberg J. Proof of principle of a generalized fuzzy Hough transform approach to peak alignment of one-dimensional 1H NMR data. *Anal Bioanal Chem*. 2007; 389(3):875–885. [PubMed: 17701402]
66. Beneduci A, Chidichimo G, Dardo G, Pontoni G. Highly routinely reproducible alignment of H-1 NMR spectral peaks of metabolites in huge sets of urines. *Anal Chim Acta*. 2011; 685(2):186–195. [PubMed: 21168568]
67. Cloarec O, Dumas ME, Trygg J, Craig A, Barton RH, Lindon JC, Nicholson JK, Holmes E. Evaluation of the orthogonal projection on latent structure model limitations caused by chemical shift variability and improved visualization of biomarker changes in H-1 NMR spectroscopic metabonomic studies. *Anal Chem*. 2005; 77(2):517–526. [PubMed: 15649048]
68. Lange E, Tautenhahn R, Neumann S, Gropl C. Critical assessment of alignment procedures for LC-MS proteomics and metabolomics measurements. *BMC Bioinf*. 2008; 9(375) Epub.
69. Nielsen NPV, Carstensen JM, Smedsgaard J. Aligning of single and multiple wavelength chromatographic profiles for chemometric data analysis using correlation optimised warping. *J Chromatogr A*. 1998; 805(1-2):17–35.
70. Tomasi G, van den Berg F, Andersson C. Correlation optimized warping and dynamic time warping as preprocessing methods for chromatographic data. *J Chemom*. 2004; 18(5):231–241.
71. Skov T, van den Berg F, Tomasi G, Bro R. Automated alignment of chromatographic data. *J Chemom*. 2006; 20(11-12):484–497.
72. Clasquin MF, Melamud E, Rabinowitz JD. LC-MS data processing with MAVEN: a metabolomic analysis and visualization engine. *Curr Protoc Bioinformatics*. 2012; 37(14.11.1–14.11.23) Epub.
73. Xia J, Mandal R, Sinelnikov IV, Broadhurst D, Wishart DS. MetaboAnalyst 2.0--a comprehensive server for metabolomic data analysis. *Nucleic Acids Res*. 2012; 40(19):W127–133. [PubMed: 22553367]
74. Pluskal T, Castillo S, Villar-Briones A, Oresic M. MZmine 2: modular framework for processing, visualizing, and analyzing mass spectrometry-based molecular profile data. *BMC Bioinf*. 2010; 11(395) Epub.
75. Vahamaa H, Koskinen VR, Hosia W, Moulder R, Nevalainen OS, Lahesmaa R, Aittokallio T, Salmi J. PolyAlign: a versatile LC-MS data alignment tool for landmark-selected and -automated use. *Int J Proteomics*. 2011; 2011:450290. [PubMed: 22084688]



76. Jeong J, Shi X, Zhang X, Kim S, Shen C. Model-based peak alignment of metabolomic profiling from comprehensive two-dimensional gas chromatography mass spectrometry. *BMC Bioinf.* 2012; 13(27) Epub.
77. Perera V, Torres ZM, Florance H, Smirnoff N, Grant M, Yang ZR. Aligning extracted LC-MS peak lists via density maximization. *Metabolomics.* 2012; 8(Supplement 1):175–185.
78. Tikunov YM, Laptinok S, Hall RD, Bovy A, Vos RCH. MSClust: a tool for unsupervised mass spectra extraction of chromatography-mass spectrometry ion-wise aligned data. *Metabolomics.* 2012; 8(4):714–718. [PubMed: 22833709]
79. Voss B, Hanselmann M, Renard BY, Lindner MS, Koethe U, Kirchner M, Hamprecht FA. SIMA: Simultaneous Multiple Alignment of LC/MS Peak Lists. *Bioinformatics.* 2011; 27(7):987–993. [PubMed: 21296750]
80. Craig A, Cloareo O, Holmes E, Nicholson JK, Lindon JC. Scaling and normalization effects in NMR spectroscopic metabolomic data sets. *Anal Chem.* 2006; 78(7):2262–2267. [PubMed: 16579606]
81. Sysi-Aho M, Katajamaa M, Yetukuri L, Oresic M. Normalization method for metabolomics data using optimal selection of multiple internal standards. *BMC Bioinformatics.* 2007; 8
82. van den Berg RA, Hoefsloot HCJ, Westerhuis JA, Smilde AK, van der Werf MJ. Centering, scaling, and transformations: improving the biological information content of metabolomics data. *BMC Genomics.* 2006; 7
83. Halouska S, Powers R. Negative impact of noise on the principal component analysis of NMR data. *J Magn Reson.* 2006; 178(1):88–95. [PubMed: 16198132]
84. Wentzell PD, Andrews DT, Hamilton DC, Faber K, Kowalski BR. Maximum likelihood principal component analysis. *J Chemom.* 1997; 11(4):339–366.
85. Hoefsloot HCJ, Verouden MPH, Westerhuis JA, Smilde AK. Maximum likelihood scaling (MALS). *J Chemom.* 2006; 20(3-4):120–127.
86. Kjeldahl K, Bro R. Some common misunderstandings in chemometrics. *J Chemom.* 2010; 24(7-8): 558–564.
87. Trygg J, Wold S. O2-PLS, a two-block (X-Y) latent variable regression (LVR) method with an integral OSC filter. *J Chemom.* 2003; 17(1):53–64.
88. Westerhuis JA, Hoefsloot HCJ, Smit S, Vis DJ, Smilde AK, van Velzen EJJ, van Duijnhoven JPM, van Dorsten FA. Assessment of PLS-DA cross validation. *Metabolomics.* 2008; 4(1):81–89.
89. Boulet JC, Roger JM. Pretreatments by means of orthogonal projections. *Chemom Intell Lab Syst.* 2012; 117:61–69.
90. Lin X, Wang Q, Yin P, Tang L, Tan Y, Li H, Yan K, Xu G. A method for handling metabolomics data from liquid chromatography/mass spectrometry: combinational use of support vector machine recursive feature elimination, genetic algorithm and random forest for feature selection. *Metabolomics.* 2011; 7(4):549–558.
91. Ramadan Z, Jacobs D, Grigorov M, Kochhar S. Metabolic profiling using principal component analysis, discriminant partial least squares, and genetic algorithms. *Talanta.* 2006; 68(5):1683–1691. [PubMed: 18970515]
92. Wongravee K, Heinrich N, Holmboe M, Schaefer ML, Reed RR, Trevejo J, Brereton RG. Variable Selection Using Iterative Reformulation of Training Set Models for Discrimination of Samples: Application to Gas Chromatography/Mass Spectrometry of Mouse Urinary Metabolites. *Anal Chem.* 2009; 81(13):5204–5217. [PubMed: 19507882]
93. Brereton RG. Consequences of sample size, variable selection, and model validation and optimization, for predicting classification ability from analytical data. *TrAC, Trends Anal Chem.* 2006; 25(11):1103–1111.
94. Geladi P, Manley M, Lestander T. Scatter plotting in multivariate data analysis. *J Chemom.* 2003; 17(8-9):503–511.
95. Vuckovic D. Current trends and challenges in sample preparation for global metabolomics using liquid chromatography-mass spectrometry. *Anal Bioanal Chem.* 2012; 403(6):1523–1548. [PubMed: 22576654]

96. Teahan O, Gamble S, Holmes E, Waxman J, Nicholson JK, Bevan C, Keun HH. Impact of Analytical Bias in Metabonomic Studies of Human Blood Serum and Plasma. *Anal Chem.* 2006; 78(13):4307–4318. [PubMed: 16808437]
97. Eriksson L, Trygg J, Wold S. CV-ANOVA for significance testing of PLS and OPLS (R) models. *J Chemom.* 2008; 22(11-12):594–600.
98. Goodpaster AM, Kennedy MA. Quantification and statistical significance analysis of group separation in NMR-based metabonomics studies. *Chemometr Intell Lab.* 2011; 109(2):162–170.
99. Dixon SJ, Heinrich N, Holmboe M, Schaefer ML, Reed RR, Trevejo J, Brereton RG. Use of cluster separation indices and the influence of outliers: application of two new separation indices, the modified silhouette index and the overlap coefficient to simulated data and mouse urine metabolomic profiles. *J Chemom.* 2009; 23(1-2):19–31.
100. Werth MT, Halouska S, Shortridge MD, Zhang B, Powers R. Analysis of metabolomic PCA data using tree diagrams. *Anal Biochem.* 2010; 399(1):58–63. [PubMed: 20026297]
101. Worley B, Halouska S, Powers R. Utilities for Quantifying Separation in PCA/PLS-DA Scores Plots. *Anal Biochem.* 2012 in press.
102. Cloarec O, Dumas ME, Craig A, Barton RH, Trygg J, Hudson J, Blancher C, Gauguier D, Lindon JC, Holmes E, Nicholson J. Statistical total correlation spectroscopy: An exploratory approach for latent biomarker identification from metabolic H-1 NMR data sets. *Anal Chem.* 2005; 77(5): 1282–1289. [PubMed: 15732908]
103. Anderssen E, Dyrstad K, Westad F, Martens H. Reducing over-optimism in variable selection by cross-model validation. *Chemometr Intell Lab.* 2006; 84(1-2):69–74.
104. Broadhurst DI, Kell DB. Statistical strategies for avoiding false discoveries in metabolomics and related experiments. *Metabolomics.* 2006; 2(4):171–196.
105. Eliasson M, Raennar S, Trygg J. From data processing to multivariate validation - essential steps in extracting interpretable information from metabolomics data. *Curr Pharm Biotechnol.* 2011; 12(7):996–1004. [PubMed: 21466461]
106. Eriksson L, Johansson E, Muller M, Wold S. On the selection of the training set in environmental QSAR analysis when compounds are clustered. *J Chemom.* 2000; 14(5-6):599–616.
107. Stone M. An Asymptotic Equivalence of Choice of Model by Cross-Validation and Akaike's Criterion. *J R Stat Soc, B.* 1977; 39(1):44–47.
108. Martens HA, Dardenne P. Validation and verification of regression in small data sets. *Chemom Intell Lab Syst.* 1998; 44(1-2):99–121.
109. Golbraikh A, Tropsha A. Beware of  $q(2)!$  *J Mol Graphics Modell.* 2002; 20(4):269–276.
110. Shao J. Linear-Model Selection by Cross-Validation. *J Am Stat Assoc.* 1993; 88(422):486–494.
111. Xu QS, Liang YZ. Monte Carlo cross validation. *Chemometr Intell Lab.* 2001; 56(1):1–11.
112. Xu QS, Liang YZ, Du YP. Monte Carlo cross-validation for selecting a model and estimating the prediction error in multivariate calibration. *J Chemom.* 2004; 18(2):112–120.
113. Ledauphin J, Le Milbeau C, Barillier D, Hennequin D. Differences in the Volatile Compositions of French Labeled Brandies (Armagnac, Calvados, Cognac, and Mirabelle) Using GC-MS and PLS-DA. *J Agric Food Chem.* 2010; 58(13):7782–7793. [PubMed: 20527953]
114. Nicholson JK, Holmes E, Wilson ID. Gut microorganisms, mammalian metabolism and personalized health care. *Nat Rev Microbiol.* 2005; 3(5):431–438. [PubMed: 15821725]
115. Sadykov MR, Zhang B, Halouska S, Nelson JL, Kreimer LW, Zhu YF, Powers R, Somerville GA. Using NMR Metabolomics to Investigate Tricarboxylic Acid Cycle-dependent Signal Transduction in *Staphylococcus epidermidis*. *J Biol Chem.* 2010; 285(47):36616–36624. [PubMed: 20861019]
116. Zhang B, Halouska S, Schiaffo CE, Sadykov MR, Somerville GA, Powers R. NMR Analysis of a Stress Response Metabolic Signaling Network. *J Proteome Res.* 2011; 10(8):3743–3754. [PubMed: 21692534]
117. IEEE Standard for Floating-Point Arithmetic. *IEEE Std 754-2008.* 2008:1–58.
118. Cortes C, Vapnik V. Support-Vector Networks. *Mach Learn.* 1995; 20(3):273–297.
119. Mahadevan S, Shah SL, Marrie TJ, Slupsky CM. Analysis of metabolomic data using support vector machines. *Anal Chem.* 2008; 80(19):7562–7570. [PubMed: 18767870]



120. Li HD, Liang YZ, Xu QS. Support vector machines and its applications in chemistry. *Chemometr Intell Lab.* 2009; 95(2):188–198.
121. Mounet F, Lemaire-Chamley M, Maucourt M, Cabasson C, Giraudel JL, Deborde C, Lessire R, Gallusci P, Bertrand A, Gaudillere M, Rothan C, Rolin D, Moing A. Quantitative metabolic profiles of tomato flesh and seeds during fruit development: complementary analysis with ANN and PCA. *Metabolomics.* 2007; 3(3):273–288.
122. Xia JM, Wu XJ, Yuan YJ. Integration of wavelet transform with PCA and ANN for metabolomics data-mining. *Metabolomics.* 2007; 3(4):531–537.
123. van der Greef J, Smilde AK. Symbiosis of chemometrics and metabolomics: past, present, and future. *J Chemom.* 2005; 19(5-7):376–386.
124. Bro R, PARAFAC. Tutorial and applications. *Chemometr Intell Lab.* 1997; 38(2):149–171.
125. Westerhuis JA, Kourti T, MacGregor JF. Analysis of multiblock and hierarchical PCA and PLS models. *J Chemom.* 1998; 12(5):301–321.
126. Forshed J, Idborg H, Jacobsson SP. Evaluation of different techniques for data fusion of LC/MS and H-1-NMR. *Chemometr Intell Lab.* 2007; 85(1):102–109.
127. Smilde AK, van der Werf MJ, Bijlsma S, van der Werff-van-der Vat BJC, Jellema RH. Fusion of mass spectrometry-based metabolomics data. *Anal Chem.* 2005; 77(20):6729–6736. [PubMed: 16223263]
128. Bras LP, Bernardino SA, Lopes JA, Menezes JC. Multiblock PLS as an approach to compare and combine NIR and MIR spectra in calibrations of soybean flour. *Chemometr Intell Lab.* 2005; 75(1):91–99.

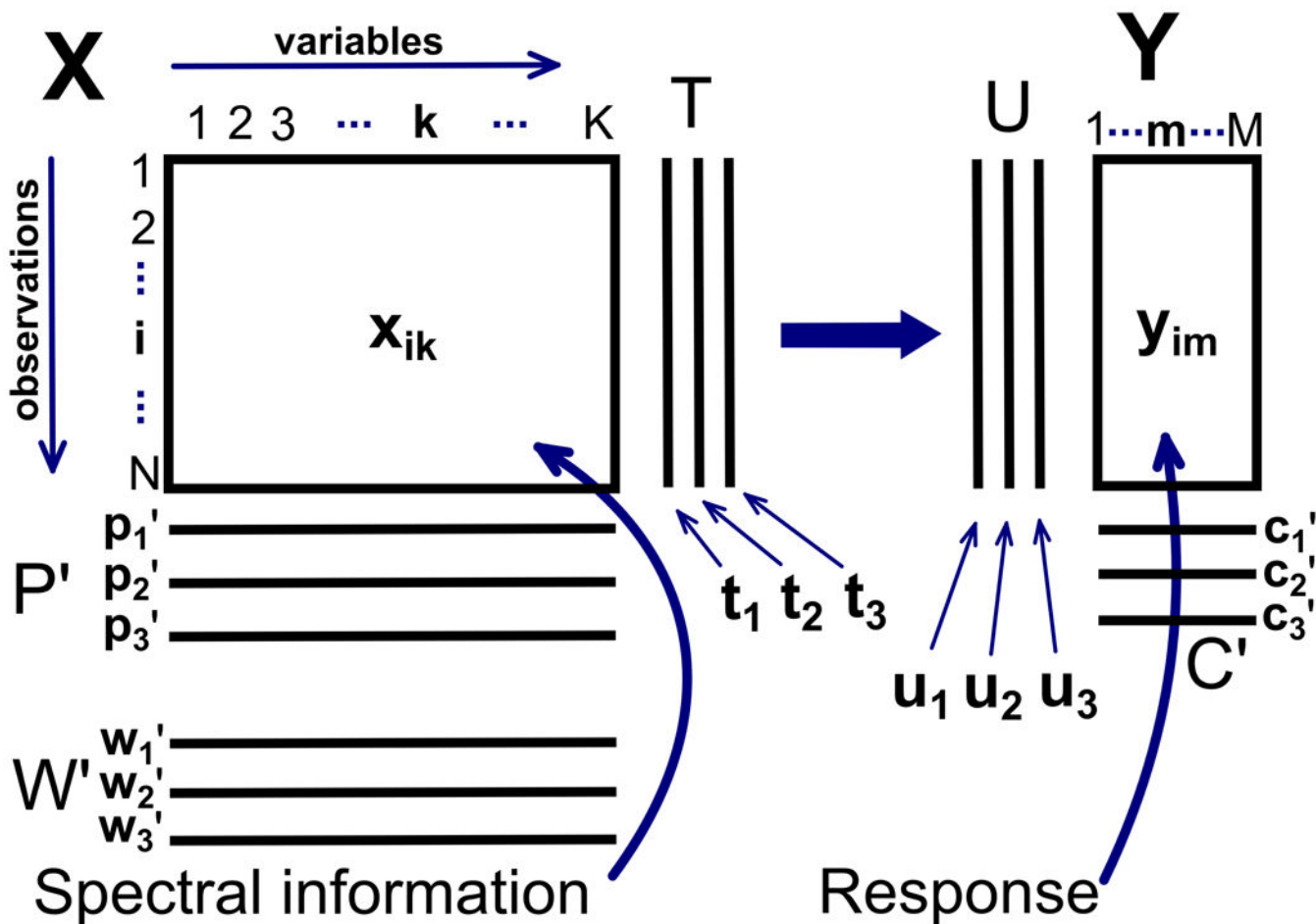


**Figure 1.** Canonical example of the data ( $X$ ) and response ( $Y$ ) matrices and decompositions thereof used by projection-based multivariate analysis algorithms. In metabolic fingerprinting applications, the data matrix will contain spectral information on its rows, such that every column will represent a single spectral frequency or bin. For supervised projections, each row of data is paired with a corresponding row in the response matrix that holds either continuously varying outputs or binary ( $n$ -ary) class memberships. The data is then decomposed into a small number of score vectors ( $t$ ) and loading vectors( $p$ ), with a corresponding weight vector ( $w$ ) used to transform rows of  $X$  to scores space. Responses are similarly decomposed into scores ( $u$ ) and loadings ( $C$ ), where  $t$  is an effective estimator of  $u$ . Adapted with permission from reference [35], (Copyright 2001 Elsevier).

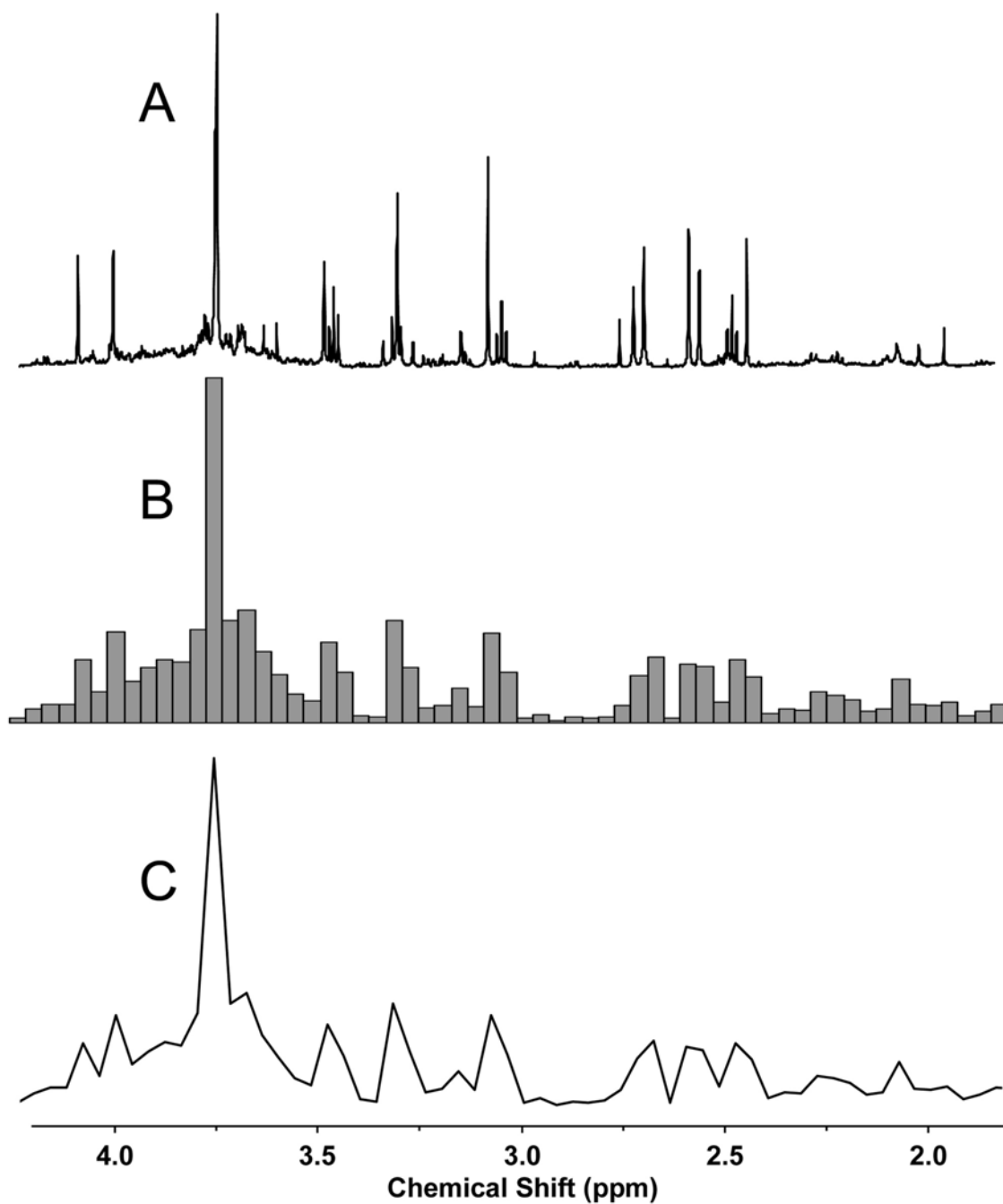


**Figure 2.** Example of the use of binning on a <sup>1</sup>H NMR spectrum of a rat urine sample, with a bin spectral width of 0.04 ppm. In this example, binning reduces the number of data variables from 65,536 to 312, facilitating multivariate analysis by PCA and PLS-DA. Reprinted with permission from reference [40], (Copyright 2007 American Chemical Society).

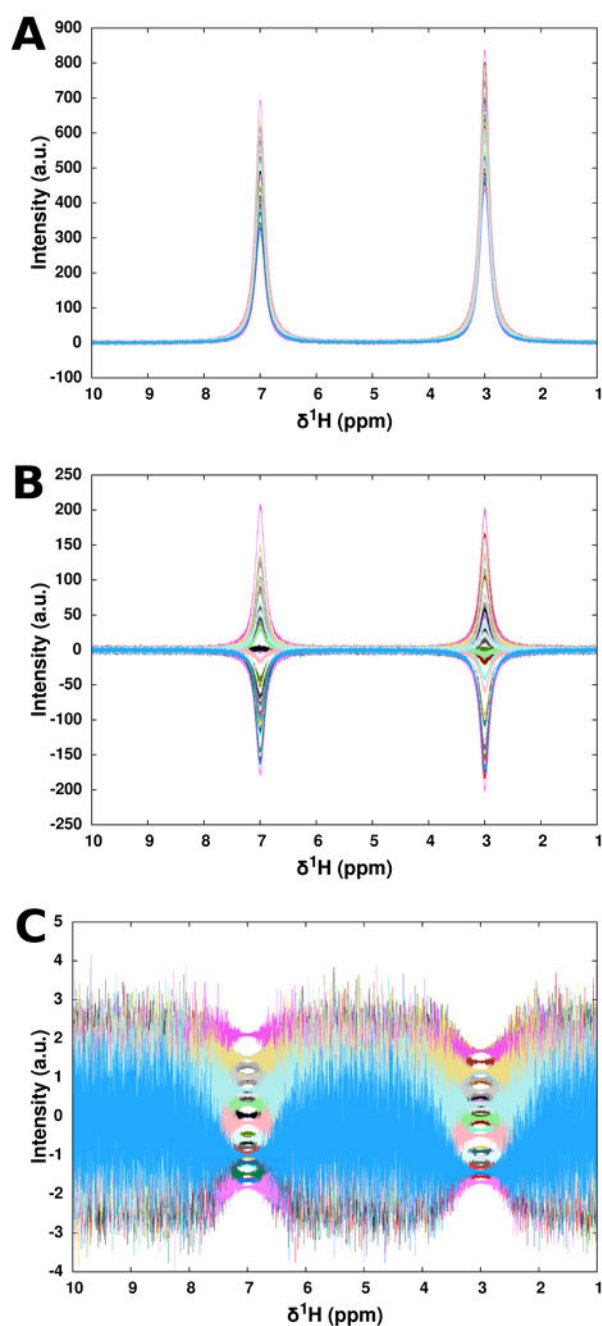


**Figure 3.** Demonstration of the effects of autoscaling to unit variance in simulated  $^1\text{H}$  NMR spectral data. (A) Set of 40 spectra containing two Lorentzian peaks having random intensities, summed with Gaussian baseline noise. (B) Spectra from above with mean-centering. (C) Spectra with mean-centering and autoscaling to unit variance, exhibiting amplification of noise in signal-free regions. Adapted with permission from reference [80], (Copyright 2006 American Chemical Society).

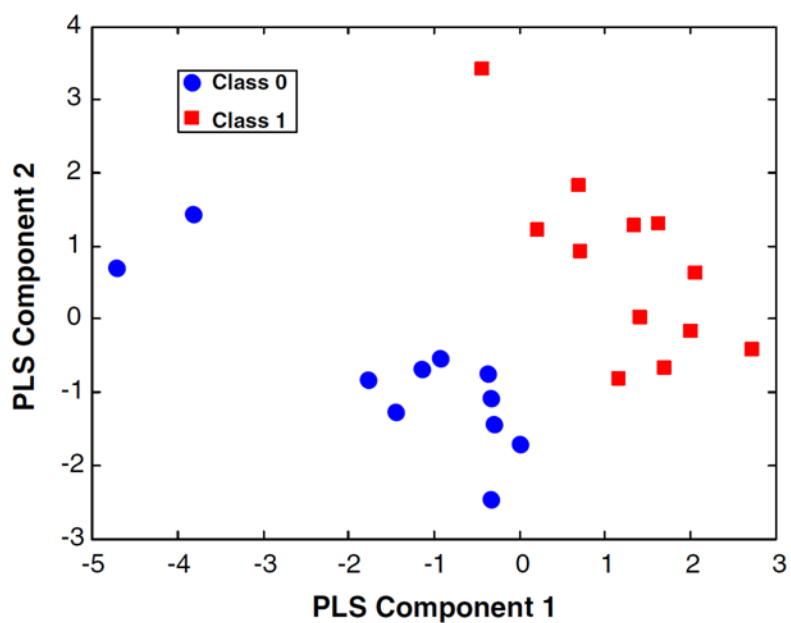


**Figure 4.** Scores from the PLS-DA discrimination of  $^1\text{H}$  NMR spectra from 23 healthy volunteers, where class labels have been randomly assigned. Internal cross-validation produces a  $Q^2$  of -0.18, clearly well below acceptable limits. Nevertheless, the scores plot displays a clear separation between classes that could lead the inexperienced practitioner to wholly false biological conclusions. Reprinted with permission from reference [88], (Copyright 2008 Westerhuis *et. al.*).

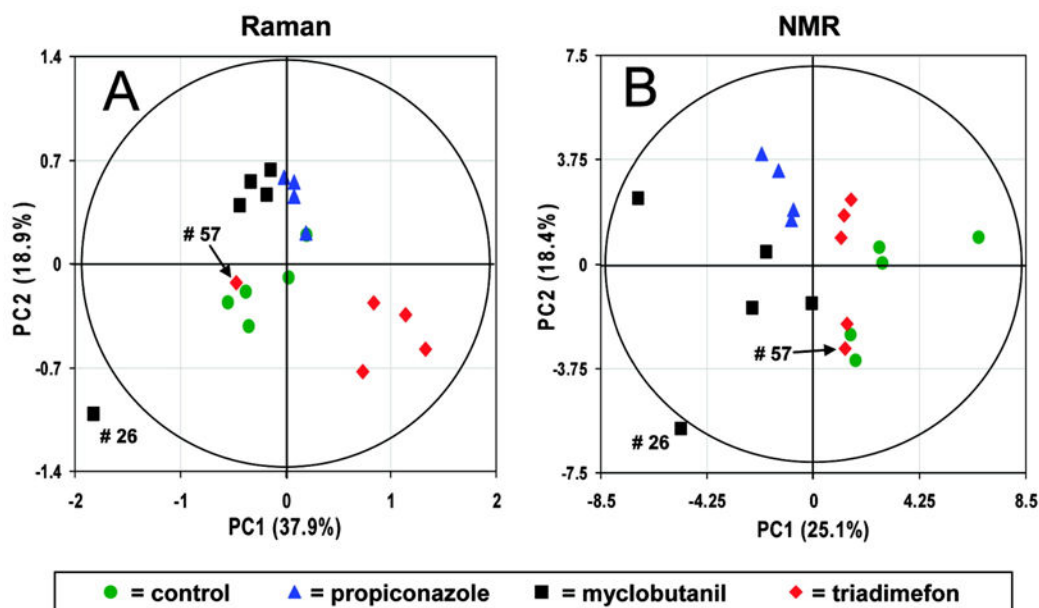


**Figure 5.** Scores from PCA decomposition of (A)  $^1\text{H}$  NMR and (B) Raman spectra of rat urine metabolites, demonstrating the use of PCA to compare within- and between-group variation datasets from complementary instrumental sources. In this example, the captured variances on each plot reflect the relative effectiveness of PCA to approximate the input data, and may not be used as a standard of comparison. Reprinted with permission from reference [40], (Copyright 2007 American Chemical Society).

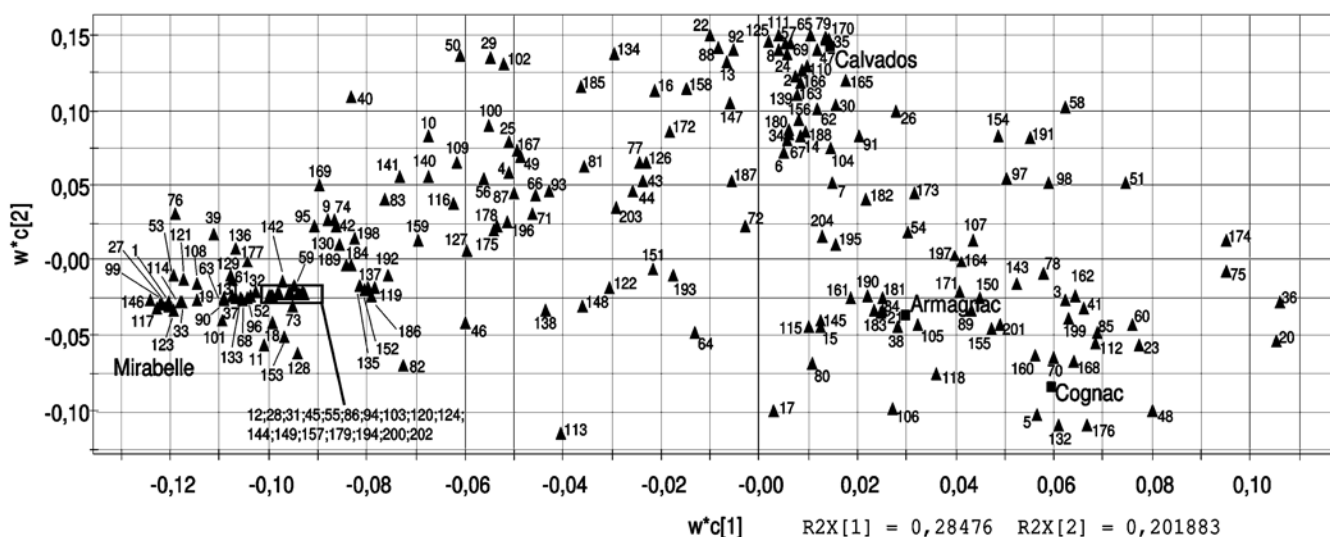


**Figure 6.**

PLS-DA loadings for volatile compound composition of French labeled brandies. Clustering patterns of variables reveal relevance of those  $X$  variables to the responses in  $Y$ . The  $Y$ -weights for each type of brandy are labeled and represented as squares, and the  $X$ -weights are represented as numbered triangles. Variable numbers relate to volatile compounds identified by GC-MS analysis, with the identity and amount of each compound may be found in reference [113]. Reprinted with permission from reference [113], (Copyright 2010 American Chemical Society).



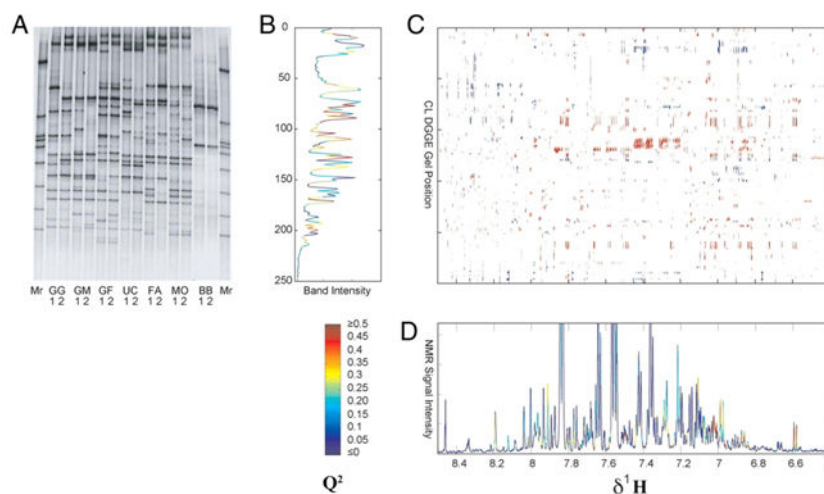


**Figure 7.** Cross-correlation analysis between the DGGE gel in (A) and collected  $^1\text{H}$  NMR spectra of urine metabolites. (B) Prediction of DGGE bands using NMR spectra. (C) Correlation matrix relating the aromatic region of collected NMR spectra to DGGE bands. Red indicates positive correlation greater than 0.7 and blue indicates negative correlation of the same magnitude or greater. (D) Prediction of the NMR spectral aromatic region based on DGGE data. Both predictions from OPLS regression are colored according to  $Q^2$  obtained from cross-validation. Reprinted with permission from reference [45], (Copyright 2008 National Academy of Sciences of the USA).

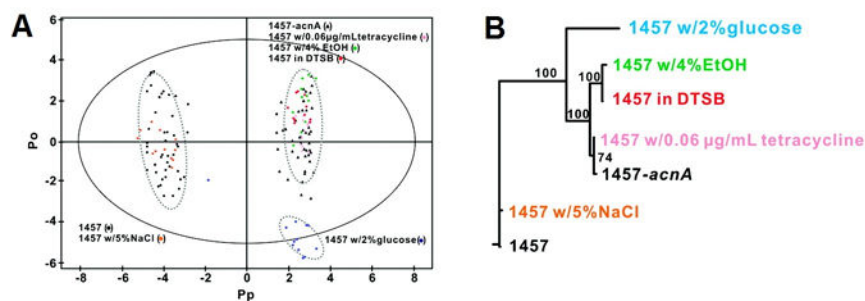


**Figure 8.**

Results of OPLS-DA modeling of the metabolomic effects of six different stressors on *S. epidermidis*. **(A)** OPLS scores of all experimental groups, showing the high observation counts for each group necessary for statistical treatment of scores. Ellipses around each group the 95% confidence regions of the groups under the assumption of normally distributed data. **(B)** Dendrogram built from OPLS scores-space data using Euclidean distances between the sample means of each group. Within-group substructure that was not forced during class discrimination is evident in the dendrogram. Group name colors in **(B)** correspond to scores colors in **(A)**. Reprinted with permission from reference [116], (Copyright 2011 American Chemical Society).

**Table 1**Listing of most commonly used data scaling methods in metabolic fingerprinting multivariate analyses.<sup>1</sup>

| Method    | Equation                                                                  | Goal                                                                          | Advantage                                                       | Disadvantage                                                   |
|-----------|---------------------------------------------------------------------------|-------------------------------------------------------------------------------|-----------------------------------------------------------------|----------------------------------------------------------------|
| Centering | $\tilde{x}_{ik} = x_{ik} - \bar{x}_k$                                     | Focus on differences, not similarities                                        | Removes offset from the data                                    | Unsuitable for heteroscedastic data                            |
| UV        | $\tilde{x}_{ik} = \frac{x_{ik} - \bar{x}_k}{s_k}$                         | Compare metabolites based on correlation                                      | All metabolites equally important                               | Inflation of measurement errors                                |
| Range     | $\tilde{x}_{ik} = \frac{x_{ik} - \bar{x}_k}{x_{k,\max} - x_{k,\min}}$     | Compare metabolites relative to biological response range                     | All metabolites equally important. Biologically related scaling | Inflation of measurement errors, sensitive to outliers         |
| Pareto    | $\tilde{x}_{ik} = \frac{x_{ik} - \bar{x}_k}{\sqrt{s_k}}$                  | Reduce relative importance of large values, partially preserve data structure | Stays closer to original measurement than UV                    | Sensitive to large fold changes                                |
| Vast      | $\tilde{x}_{ik} = \frac{x_{ik} - \bar{x}_k}{s_k} C \frac{\bar{x}_k}{s_k}$ | Focus on small fluctuations                                                   | Aims for robustness, uses prior group knowledge                 | Not suited for large induced variation without group structure |
| Level     | $\tilde{x}_{ik} = \frac{x_{ik} - \bar{x}_k}{x_k}$                         | Focus on relative response                                                    | Suited for biomarker identification                             | Inflation of measurement errors                                |

<sup>1</sup>Variable subscripts reflect conventions shown in Figure 1, with the mean of the  $k$ -th variable in  $\mathbf{X}$  represented by  $\bar{x}_k$  and its deviation represented by  $s_k$ , the sample standard deviation. Reprinted with permission from reference [82], (Copyright 2006 van den Berg *et. al.*).